Measurement Science and Technology

Meas. Sci. Technol. **25** (2014) 105304 (6pp)

doi:10.1088/0957-0233/25/10/105304

A calibration technique to correct sensor drift issues in hot-wire anemometry

K M Talluru[1], V Kulandaivelu[2], N Hutchins[3] and I Marusic[3]

[1] School of Engineering, The University of Newcastle, NSW 2308, Australia
[2] Department of Mechanical Engineering, The University of Utah, UT 84112, USA
[3] Department of Mechanical Engineering, The University of Melbourne, VIC 3010, Australia

E-mail: murali.talluru@newcastle.edu.au

Abstract

Accurate calibration is imperative to obtain reliable flow measurements using hot-wire anemometry. Calibration errors owing to temperature drift, wire degradation, changes in ambient conditions etc can lead to substantial uncertainties in hot-wire measurements. A new calibration procedure is implemented here to account for most forms of drift that are typically encountered during high quality flow measurements using hot-wires. The method involves obtaining single point recalibrations of the hot-wire (in the free-stream) at regular intervals during the course of an actual experiment, and using these during post-processing to correct for any drift encountered. Unlike many other existing schemes, this proposed calibration correction method is not solely restricted to correcting temperature drift.

Keywords: hot-wire anemometry, hot-wire drift, calibration technique

(Some figures may appear in colour only in the online journal)

1. Introduction

Hot-wire anemometry (HWA) is a well-established technique that is used to obtain the time series information of velocity fluctuations in turbulent flows. With this technique, the velocity measurements are indirectly inferred from changes to the heat transfer from a small heated wire of diameter $O(\mu m)$ placed in the flow. The accuracy of this method is heavily dependent on the accuracy of the calibration which relates measured heat-transfer from the hot-wire to velocity. Any errors in calibration give rise to greater levels of uncertainty in the hot-wire measured velocity. Calibration drift may be caused due to changes in the ambient conditions of the flow such as temperature [4], humidity [5], and pressure; wire degradation due to incomplete cleaning [14], electro-migration [15]; dust particles in the flow [3] and wire fouling [16]. Several correction schemes are available for calibrations (e.g. [1, 2, 5, 6, 9, 11, 13]). Though there are exceptions [5, 9], most of these have attempted to correct solely for the fluid temperature drift. In these methods, the temperature correction has typically been carried out by either (i) obtaining multiple calibration curves at different temperatures and using interpolation schemes to cover the intermediate temperatures or (ii) applying some analytical correction based on King's law. There is no single available calibration technique that accounts for all sources of drift in a given experiment. To address this issue, a new calibration technique is developed here that is capable of correcting different forms of drift issues and can be applied universally in all types of hot-wire anemometry systems. We believe that this method is superior in the sense that it does not assume any heat-transfer formulations and also does not require multiple full calibration curves at different temperatures. In addition, it is easy to integrate into existing hot-wire experiments. In simple terms, the method requires relocating the hot-wire sensor adjacent to the calibrated device (typically a Pitot-static tube) at regular intervals during the course of an experiment to obtain a single intermediate calibration point. This is then used during the post-processing stage to generate intermediate calibration curves which subsequently act as an on-the-fly correction accounting for most types of drift that the hot-wire might experience during the experiment. The proceeding section gives a detailed description of the technique which is hereafter referred to as intermediate single point recalibration (ISPR).

For this manuscript, the ISPR technique and the resulting improvement in accuracy is demonstrated for a boundary layer

traverse experiment. However, we feel that this technique could offer similar advantages in many HWA experiments.

2. Intermediate single point recalibration

The hot-wire is calibrated statically against a Pitot-static tube located at the centreline of the tunnel in the undisturbed free-stream. Calibrations are performed before and after each boundary layer traverse (referred to here as pre- and post-calibrations). Thus far, this is relatively standard technique for hot-wire operation. To account for calibration drift during the boundary layer experiments, the probe is periodically traversed to the free-stream during the course of the boundary layer profile measurement. This excursion to the free-stream occurs every Nth measurement point. For the example shown in figure 1, $N = 6$. At each free-stream excursion, the mean voltage measured by the hot-wire and the mean velocity measured by the Pitot-static tube provides an additional *recalibration* point at various intervals during the boundary layer traverse. Effectively, this means that for every N measurements[4] during the boundary layer traverse (which typically consists of approximately 50 logarithmically spaced measurement stations), the probe is recalibrated.

This process is illustrated in figure 1. The top plot (a) shows a time-line for a typical laboratory boundary layer experiment. Time $t = 0$ represents the start of the traverse experiment. The pre-calibration was performed some time (approximately 30 minutes) prior to this. The post-calibration was performed after the boundary layer traverse experiment, at approximately $t = 220$ minutes. Also represented on figure 1(a) by the black dots and the grey line, are the boundary layer measurements and the traverse path respectively. In this example, the probe was traversed to 50 logarithmically spaced stations from $0.2 < z < 500$ mm. The traverse shown in figure 1(a) is represented as voltage against time and one can easily discern the characteristic mean velocity profile. After the first six measurements, the probe (which was then at $z \approx 0.6$ mm) is traversed upwards to the free-stream (at $z = 500$ mm), and the first *recalibration* point is obtained. The probe then returns to the next traverse point ($z = 0.7$ mm) and the traverse measurment resumes. Free-stream recalibration is performed for every sixth measurement thereafter. Since the free-stream velocity of the tunnel is held constant throughout the measurement run, any variation in the measured mean voltage E at these recalibration points is indicative of calibration 'drift' (for the schematic shown in figure 1, an approximate linear variation is represented during the run). The new voltage measured at the recalibration point E_i is then used to calculate the proportional drift (R) of the given recalibration point relative to the total drift between the pre- and post-calibrations,

$$R\,|_i = \frac{(E_i - E_{\mathrm{pre}})\,|_{U_{\infty i}}}{(E_{\mathrm{post}} - E_{\mathrm{pre}})\,|_{U_{\infty i}}}, \qquad (1)$$

where i represents the ith recalibration point, and E_{pre} and E_{post} are evaluated from the pre- and post-calibration curves (using a third-order polynomial fit) at the freestream velocity corresponding to the ith calibration point (U_{∞_i}). This ratio $R|_i$ is subsequently used to generate an intermediate calibration curve (E_{int}) across the full range of calibration velocities U using,

$$E_{\mathrm{int}}\,|_U = R|_i * (E_{\mathrm{post}}|_U - E_{\mathrm{pre}}|_U) + E_{\mathrm{pre}}|_U. \qquad (2)$$

This yields a new calibration curve $E_{\mathrm{int}}|_i$ versus U that passes through the recalibration point. This process is illustrated for the 3rd recalibration point in figure 1(b) (and inset). Hence a new calibration curve (shown by the grey dashed line in figure 1(b)) is produced that can be considered correct at the time of each free-stream recalibration. For the intervening measurements, between single point recalibrations, a linear interpolation in time is employed.

This process relies on accurate wall-normal positioning, which enables us to interrupt a wall-normal boundary layer traverse, relocate the probe to the free-stream for the 'recalibration' point, and then return accurately to the original position within the turbulent boundary layer. This is achieved in the current study by using a computer-controlled servo-motor with a Renishaw RGH24 linear encoder, offering a resolution of 1 μm (0.04 wall units at $Re_\tau = 6200$ for the current measurements). This technique also relies upon the assumption that the free-stream recalibration points should vary in time as a smooth function. Any erratic jumps or step changes cannot be accounted for reliably during post-processing and in these instances the experimental run should be discarded.

3. Experiment and discussion

To evaluate the calibration procedure described in the previous section, experiments are conducted in the high Reynolds number boundary layer wind tunnel (HRNBLWT) facility at the University of Melbourne. Measurements are made at a friction Reynolds number, $Re_\tau = 6200$, achieved with a free-stream velocity of 15 m s^{-1} at a streamwise location 12.8 m downstream of the tripped inlet to the working section. More details of the facility can be found in [7, 8, 10]. It is noted that this is a state-of-the-art facility where great lengths have been taken to ensure high quality conditions. The probes used for these experiments are modified Dantec 55P15 type with a prong spacing of 1.5 mm. The sensor is formed from the etched portion of a Wollaston wire to reveal a 2.5 μm diameter Platinum core of length 0.5 mm (corresponding to an $l^+ \approx 17$).

To test the veracity of the proposed calibration procedure, three experimental runs are conducted consecutively over a period of 18 hours. The first calibration is conducted at $t = 0$ (start), followed by experimental run 1 that lasted for 5 hours. A post-calibration was performed after run 1, which also acted as the pre-calibration for run 2. Run 2 was carried out between 6 and 11 hours from the start and in a similar pattern, run 3 was completed at 17 hours. A final calibration was carried out at $t = 18$ hours. It is noted that the temperature only changed by 0.2 °C, 0.5 °C and 0.3 °C during runs 1, 2 and 3 respectively. The temperature is measured continuously in the undisturbed free-stream for the entire duration of the experiment using a DP25 series

[4] The relationship between N and the overall accuracy of the technique will be discussed in section 3.

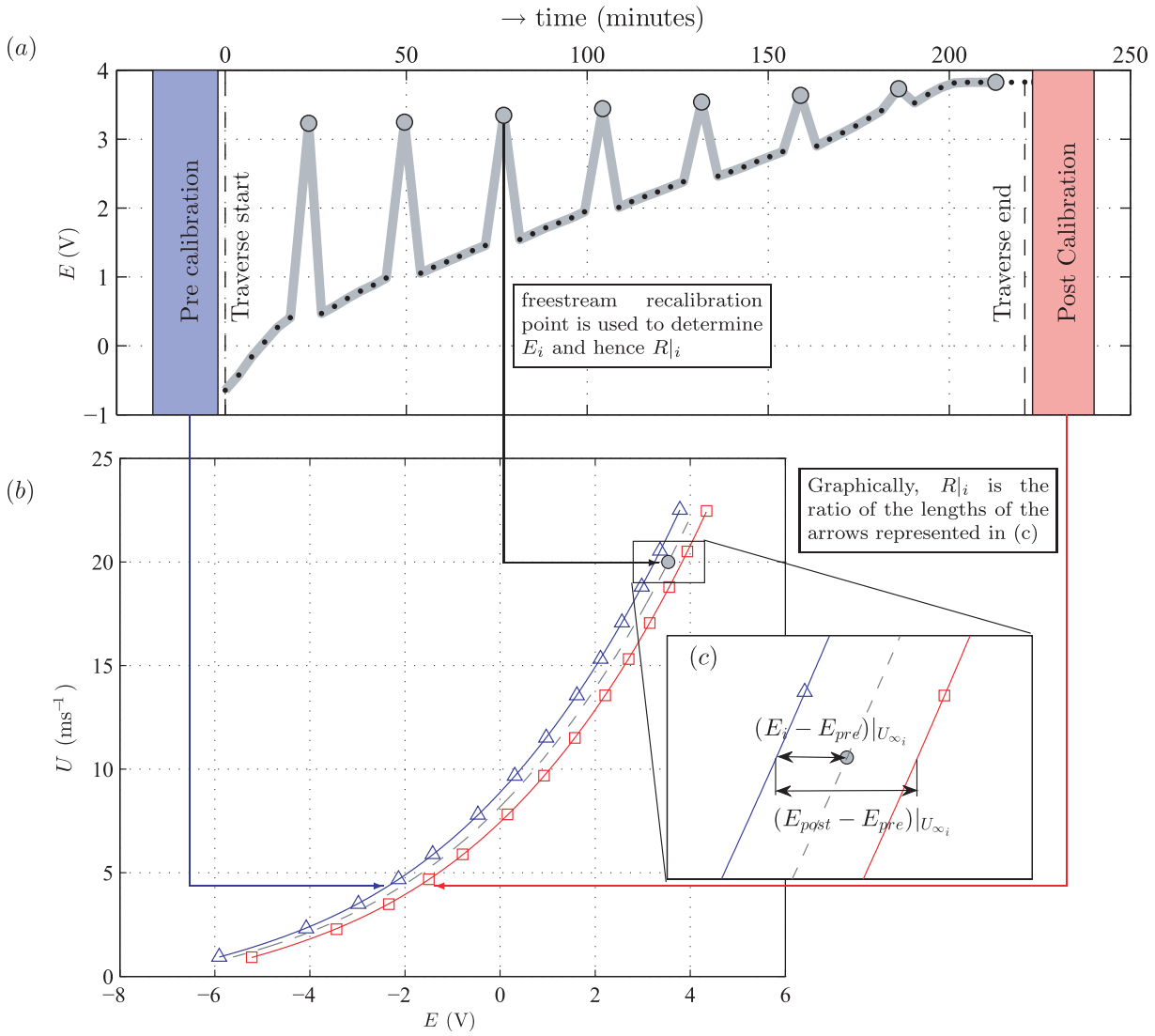

Figure 1. A schematic figure illustrating an example of the intermediate single point recalibration (ISPR) method applied in this case to a wall-normal traverse in a turbulent boundary layer. (*a*) A time line of the experiment. Blue and red shaded regions show the time of the pre- and post-calibrations respectively. The black dashed lines show the start and end times of the boundary layer traverse experiment. (•) show the individual traverse measurements of mean voltage, (●) show the free-stream 'recalibration' points. (*b*) shows the (△) pre and (□) post-calibration curves. The inset (*c*) shows a detail of the intermediate calibration curve (dashed grey line). In this example, the ratio $R|_i$ is obtained from the 3rd free-stream recalibration point.

thermocouple from Omega, USA with a resolution of 0.1 °C. The consistency in the measurements is taken as an indicator of the ability of the calibration procedure to deal with drift issues. Here, we convert the time-series hot-wire voltage signals from the experiment into fluctuating velocity using five different calibration procedures as summarised in table 1. They are: (I) using only the pre-calibration, (II) using only the post-calibration, (III) where an intermediate calibration curve is constructed based on a measured temperature during the experiment, relative to T_{pre} and T_{post}. (IV) Linear interpolation between the pre- and post-calibrations with time and finally (V) the ISPR method as described in section 2. In this study, the calibration curves are generated by fitting a third-order polynomial between the measured voltage and velocites during the pre- and post-calibrations. The intermediate calibration curves are produced by using a cubic spline interpolation scheme in accordance to equations (1)–(4).

Table 1. Description of various calibration methods used for comparison in this study.

Method number	Description
I	Using only the pre-calibration
II	Using only the post-calibration
III	Interpolation between the pre- and post-calibrations based on measured temperature relative to T_{pre} and T_{post}
IV	Linear interpolation between the pre- and post-calibrations with time
V	Using the intermediate single point recalibration (ISPR) method

Methods III and IV can be better explained using figure 1(*b*) where intermediate calibration curves are generated using a different proportional drift R, which is obtained using either interpolation with measured temperature (III) or time (IV),

$$R_{j_{[III]}} = \frac{T_j - T_{\text{pre}}}{T_{\text{post}} - T_{\text{pre}}}, \tag{3}$$

where T_{pre} is the temperature of pre-calibration, T_{post} is the temperature of post-calibration and T_j is the temperature at an intermediate time during the experiment (in this example $j = 1{:}M$, where $M = 50$ is the number of measurement stations within the boundary layer traverse). Similarly, in method IV, R is obtained by interpolating with time as,

$$R_{j_{[IV]}} = \frac{t_j - t_{\text{pre}}}{t_{\text{post}} - t_{\text{pre}}}. \tag{4}$$

where t_{pre} is the time at which the pre-calibration was conducted, t_{post} is the time of the post-calibration and t_j is the time of an individual measurement within the experiment. These revised values of R are then used in equation (2) to produce intermediate calibration curves for the jth measurement.

Figures 2(*a*) and (*b*) show the comparison of typical mean velocity and turbulence intensity profiles in three experimental runs obtained using all the five calibration procedures. The results are shown using a dashed line, a solid line and a dotted line for experimental runs 1, 2 and 3 respectively. The mean quantities have been normalised using free-stream velocity (U_∞) and boundary layer thickness (δ) to minimise the errors concomitant with determining friction velocity U_τ from the mean velocity profile. It is observed that there is a good collapse in the velocity profiles in cases (IV) and (V) while the other three methods (I, II and III) have produced inconsistent results. To better assess the repeatability of the calibration techniques, we used the scatter in the mean velocity (U) as an indicator (where the smaller the scatter, the better the performance of the calibration correction). At first, a representative mean velocity profile (U_{avg}) is obtained for each method by averaging the velocity profiles across the three experimental runs as, $U_{\text{avg}} = (U_1 + U_2 + U_3)/3$, where subscripts 1, 2 and 3 represent the three runs. Then, the scatter in U is obtained as the mean of the absolute error in U calculated about U_{avg} and is shown as a percentage in figure 2(*c*) as a function of wall-normal position. It is clear that methods IV and V have performed equally well having a maximum scatter of 1% across the boundary layer, while the other methods have relatively larger scatter.

The deficiencies in methods I-III can be explained as follows. In typical experiments such as those in the current study, there is a noticeable drift in the hot-wire voltage due to the long duration of the experiment. Hence, using pre- or post-calibration (methods I or II alone) would not be able to correct for the drift. Both these methods could potentially be applied in cases where the experiment is short and the drift in hot-wire voltage is negligible. However, for long experiments, method I would be expected to be most accurate at the beginning of the experiment, while method II will become more accurate towards the end. Indeed, such behavior is evident in figure 2(*c*). In method III, a linear interpolation scheme is applied based on the temperature measurement of the flow. This method makes an explicit assumption that temperature change is the only source of calibration drift, and if we account for this, data are reliably

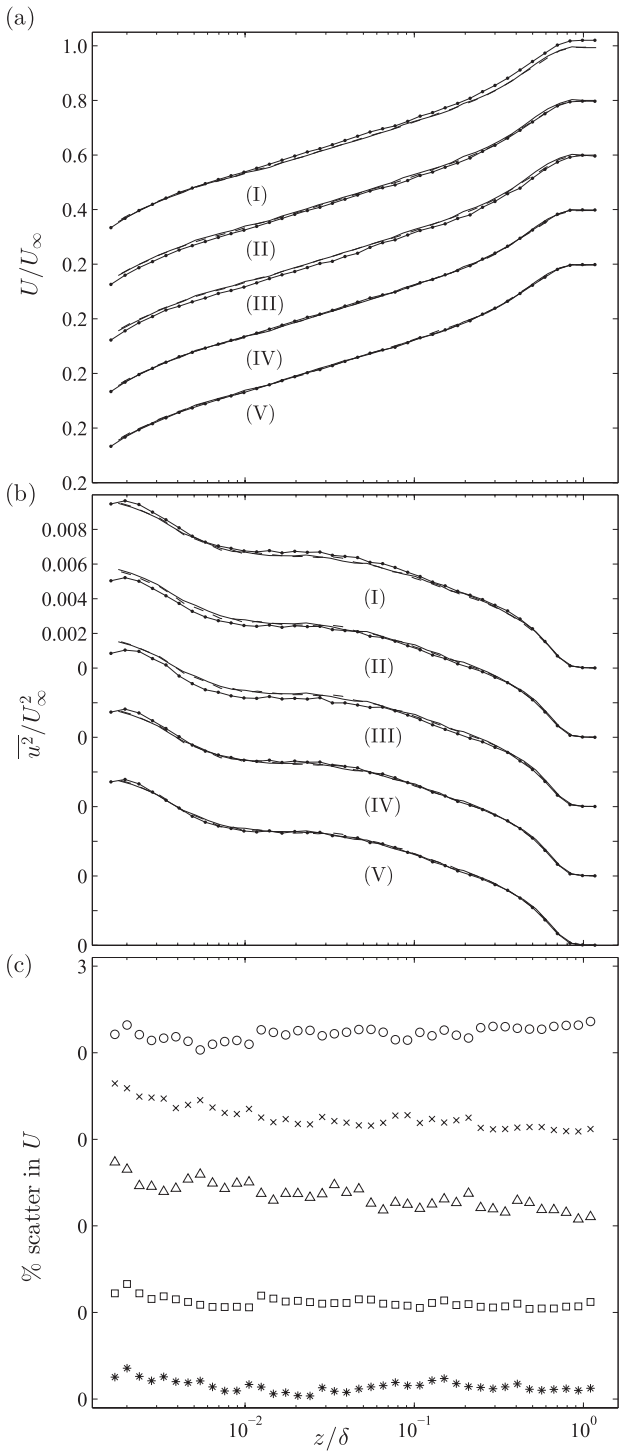

Figure 2. Comparison of (*a*) mean velocity and (*b*) turbulence intensity profiles obtained using five different calibration procedures I–V in three experimental runs; dashed line—run1; solid line—run2; dotted line—run3. (*c*) Percentage scatter in U calculated about the mean velocity (U_{avg}) across the three experimental runs; ○—method I; ×—method II; △—method III; □—method IV; ∗—method V.

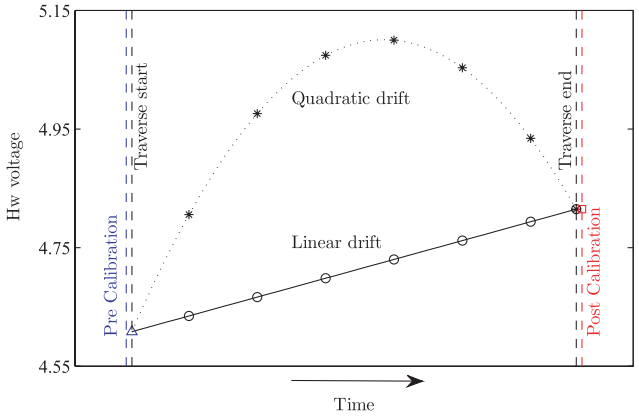

Figure 3. Simulated hot-wire drifts—(○) linear and (∗) quadratic.

corrected. In reality, as discussed in section 1, calibration drift can occur for a number of reasons. In the current study, the temperature of the flow only changed from 22.4 °C to 23.4 °C over a period of 18 h. The failure of method III to adequately collapse the three experimental runs is indicative that in this case other sources of drift are active and that accounting for temperature change alone is insufficient.

An interesting result we noticed in these results is that methods IV and V worked equally well. They seem to produce very consistent results both in the mean velocity and turbulence intensity profiles. Upon careful observation of the recalibration points, we noted that the hot-wire drifted in an approximately linear fashion between the pre- and post-calibrations for all the three experimental runs. In this instance, method IV is approximately equivalent to method V. This is because the ISPR method can be understood as a more discretized version of method IV. In method IV, we use a linear interpolation in time between the pre and the post calibrations with the implicit assumption that the hot-wire drifted in a linear fashion during the 50 point measurement of the boundary layer. While in the ISPR method, we assume a linear drift in hot-wire voltage between every two consecutive intermediate recalibration points that are only N measurement points apart in time. Obviously then methods IV and V are increasingly equivalent when either (i) N becomes very large or (ii) the drift from pre-calibration to post-calibration (as indicated by the intermediate recalibration points) is approximately linear (as is shown for the example in figure 3).

To elucidate further the distinction between methods IV and V, we performed simulations on the experimental data where two types of drift are artificially imposed on the hot-wire data and calibration procedures IV and V are implemented to evaluate which of the two techniques produced consistent results. Here, we implemented the hot-wire drift in a linear and a quadratic trend which are better illustrated in figure 3, where the variation of hot-wire voltage is shown as a function of time between the pre- and the post-calibrations. The intermediate free-stream monitored hot-wire voltages are marked on figure 3 by the (○) and (∗) symbols for the linear and quadratic drift respectively. The outcome of this analysis is shown in figure 4, where the comparison of mean velocity and turbulence intensity profiles using methods IV and V is presented.

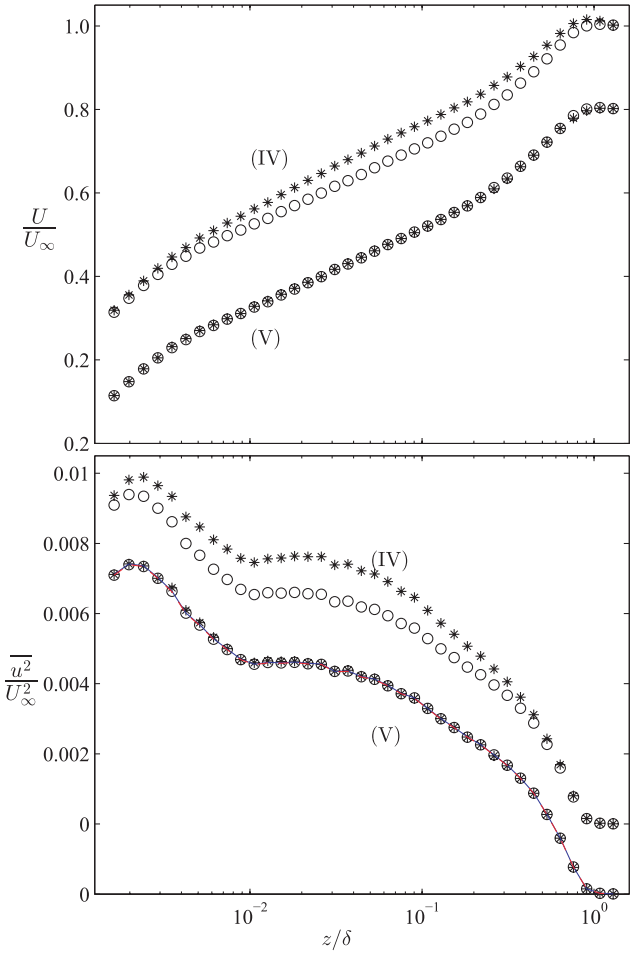

Figure 4. Comparison of mean velocity and turbulence intensity profiles using methods IV and V for the simulated hot-wire drifts linear (○) and quadratic (∗). Results computed with $N = 1$ and cubic spline fit are shown respectively by dashed red line and blue line.

It is clear that the linear interpolation in time (method IV) cannot adequately account for the non-linear quadratic drift in the hot-wire voltage while the ISPR method produces consistent results in both kinds of drift. Such a non-linear drift in hot-wire voltage is often observed during experimental runs, for example, in field experiments or for long laboratory experiments where the room temperature is uncontrolled and follows the diurnal cycle of atmospheric temperature change.

Despite the success of method V, small inconsistencies can arise in certain cases in the results obtained using the ISPR technique. For example, when the hot-wire drift pattern follows a higher order polynomial. This is because the method still assumes a linear change in the hot-wire voltage between two successive free-stream recalibrated points. There are further refinements that can deal with these remaining sources of error. (1) We could reduce N. The assumed linear variation between successive recalibration points will improve in accuracy as $N \to 1$. However, this approach will add greatly to the overall duration of the measurement (since there are more excursions to reposition the HWA sensor next to the calibration device) and the positional certainty (in z) for the experiment may be compromised due to the frequent repositioning. (2) We could fit a functional form to the recalibration points (higher order polynomial or cubic spline

fit). For the example shown in figure 4, both methods (1) and (2) have been attempted (shown by the red and blue curves respectively). In this case there is very little improvement in accuracy over the $N = 6$ case, with simple linear interpolation between successive recalibration points. However, in situations where the drift was following a higher order curve, such techniques could prove useful. As a final point, it should be noted that the ISPR method is incapable of dealing with sudden step changes in hot-wire voltage regardless of the interpolation scheme used between the recalibration points. There is an implicit assumption that drift occurs smoothly in time between these points. Sudden step changes could be caused by a skipping wire [12] or severe impacts with contaminants [3]. In this case, the ISPR method provides an additional sanity check on the quality of the data. Those situations where a smooth function fails to describe the recalibration points are indicative of some wider problem with the HWA, that no amount of correction or post-processing is likely to successfully deal with. In these situations the data should be discarded. In addition, the ISPR technique would fail in situations where the pre- and post-calibration curves in figure 1(*b*) perfectly collapse onto each other. This can be possible when the hotwire drifts in one direction for some duration of the experiment and returns back to its original state. In such a scenario, the denominator in equation (1), $(E_{\text{post}} - E_{\text{pre}})|_{U_\infty} \rightarrow 0$ and the numerator $(E_i - E_{\text{pre}})|_{U_\infty}$ is a non-zero quantity causing the value of $R|_i \rightarrow \infty$. However, it should be noted that such a scenario would be extremely rare, and even if the pre- and post-calibration curves were close to each other, the technique should still work as long as they were not identical or did not intersect. Furthermore, even if such a situation were to occur, the ISPR technique would at least alert the user to this drift scenario. In the absence of intermediate freestream monitoring, such a drift pattern would be impossible to discern. In fact, the user would incorrectly assume that drift had not occured during the experiment (because the difference between pre- and post-calibrations is the principal method through which many users assess the drift).

4. Conclusions

A calibration procedure has been successfully implemented that is shown to work consistently well in correcting most drift profiles observed in hot-wire anemometry during boundary layer experiments. It is observed that conventional calibration procedures will fail in certain drift situations, while the ISPR method produces more reliable results. ISPR appears to be a promising technique that could be applied in facilities wherever accurate traversing systems are used.

Acknowledgments

The authors gratefully acknowledge the Australian Research Council for the financial support of this work. The referees are thanked for their insightful comments.

References

[1] Bruun H H 1995 *Hot Wire Anemometry: Principles and Signal Analysis* (Oxford: Oxford University Press)
[2] Cimbala J M and Park W J 1990 A direct hot-wire calibration technique to account for ambient temperature drift in incompressible flow *Exp. Fluids* **8** 299–300
[3] Collis D C 1952 The dust problem in hot-wire anemometry *Aeronaut. Q.* **4** 93–102
[4] Comte-Bellot G 1976 Hot-wire anemometry *Annu. Rev. Fluid Mech.* **8** 209–31
[5] Durst F, Noppenberger S, Still M and Venzke H 1996 Influence of humidity on hot-wire measurements *Meas. Sci. Technol.* **7** 1517
[6] Hultmark M and Smits A J 2010 Temperature corrections for constant temperature and constant current hot-wire anemometers *Meas. Sci. Technol.* **21** 105404
[7] Hutchins N, Nickels T B, Marusic I and Chong M S 2009 Hot-wire spatial resolution issues in wall-bounded turbulence *J. Fluid Mech.* **635** 103–36
[8] Kulandaivelu V 2012 Evolution of zero pressure gradient turbulent boundary layers from different initial conditions *PhD Thesis* The University of Melbourne
[9] Nekrasov Y P and Savostenko P I 1991 Pressure dependence of hot-wire anemometer readings *Meas. Technol.* **34** 462–5
[10] Nickels T B, Marusic I, Hafez S and Chong M S 2005 Evidence of the k_1^{-1} law in a high Reynolds number turbulent boundary layer *Phys. Rev. Lett.* **95** 074501
[11] Perry A E 1982 *Hot Wire Anemometry* (Oxford: Oxford University Press)
[12] Perry A E and Morrison G L 1971 Vibration of hot-wire anemometer filaments *J. Fluid Mech.* **50** 815–25
[13] Tropea C, Yarin A L and Foss J F 2007 *Springer Handbook of Experimental Fluid Mechanics* Vol 1 (Berlin: Springer)
[14] Willmarth W W and Bogar T J 1977 Survey and new measurements of turbulent structure near the wall *Phys. Fluids* **20** 9–21
[15] Willmarth W W and Sharma L K 1984 Study of turbulent structure with hot wires smaller than the viscous length *J. Fluid Mech.* **142** 121–49
[16] Wyatt L A 1953 A technique for cleaning hot-wires used in anemometry *J. Sci. Instrum.* **30** 13